CrossMark

A New Method for Measuring Infrared Band Strengths in H₂O Ices: First Results for OCS, H₂S, and SO₂

Yukiko Y. Yarnall[1,2] and Reggie L. Hudson[1]

[1] Astrochemistry Laboratory, NASA Goddard Space Flight Center, Greenbelt, MD, 20771 USA; reggie.hudson@nasa.gov
[2] Universities Space Research Association, Greenbelt, MD 20771, USA

Abstract

Infrared (IR) band strengths are needed to extract accurate molecular abundances from astronomical observations of interstellar and solar system ices. However, laboratory measurements of such intensities often have required multiple assumptions about ice composition and thickness. Here we describe a method that circumvents most of the common assumptions and uncertainties in IR band-strength determinations. We have applied the method to measure IR band strengths of OCS, H₂S, and SO₂ in the absence and presence of H₂O ice at 10 K, the first measurements of their type. Our results show for the first time that the presence of H₂O makes little difference in IR intensities for these three sulfur-containing molecules' strongest IR features. The immediate application will be to laboratory studies of low-temperature chemistry of interstellar and cometary ices.

1. Introduction

The accurate determination of molecular abundances in extraterrestrial solids using infrared (IR) spectroscopy is a long-standing challenge to both interstellar and planetary astronomers. The usual approach to the problem involves Equation (1), where N (in molecules cm^{-2}) is the desired column density of a molecule or ion responsible for an IR absorption, the numerator on the right is the optical depth (τ) of an ice's absorbance feature integrated over wavenumber ($\tilde{\nu}$ in cm^{-1}), the ice being either extraterrestrial or a laboratory analog, and the denominator is a reference IR band strength A' (in cm molecule^{-1}) from laboratory measurements:

$$N = \frac{\int_{\text{band}} (\tau) d\tilde{\nu}}{A'}. \tag{1}$$

Extensive financial and human resources have been devoted to observatory and spacecraft determinations of this fraction's numerator, but much less attention has been paid to the denominator's A' on which the calculation of the column density N rests.

In this brief paper, we describe our recent development and application of an apparently novel method for determining IR band strengths (A') of molecules in mixed molecular ices, the method relying on laboratory data of the type (i.e., density, refractive index) we recently published here (Hudson et al. 2020). We have used results obtained with our method to address the applicability of IR band strengths of relatively simple ices to the more-complex solids expected in interstellar and planetary environments. More specifically, we compare spectral intensities for several strong IR features of the sulfur-containing molecules OCS, H₂S, and SO₂ in the absence and presence of H₂O ice. The method we describe not only delivers

accurate results, but it avoids many of the unchecked assumptions that often are made in such laboratory work.

The interest in sulfur among laboratory astronomers is easy to document from just our own work. One of our earliest papers concerned cometary S₂, which was followed by a study of H₂S and SO₂ on icy satellites (Moore et al. 1988, 2007). Later work covered OCS formation in interstellar ices, Jovian NH₄SH, and the solid-phase IR spectra of four thiols (Ferrante et al. 2008; Hudson 2016; Loeffler et al. 2016; Hudson & Gerakines 2018). Many other laboratory studies concerning extraterrestrial sulfur can be found in the publications referenced in the present paper.

Studies of sulfur in astronomical environments are just as easy to locate. Known interstellar molecules include OCS, H₂S, and SO₂, among others. For a summary and original references, see McGuire (2018). The only reasonably secure identification of sulfur in interstellar ice still seems to be that of OCS by Palumbo et al. (1997). Kama et al. (2019) published an extensive study of refractory sulfur in protoplanetary disks. Within the solar system, reports have been published about sulfur species in comets (A'Hearn et al. 1983), on Europa (Carlson et al. 1999), on Mars (Heinz & Schulze-Makuch 2020), in carbonaceous meteorites (Sephton 2002), and in atmospheres of the gas giants (e.g., Irwin et al. 2018). Among astrobiologists, sulfur is valued as a key bio-element in several amino acids (Brosnan & Brosnan 2006).

In this paper, the laboratory method we describe is aimed at experimental work on the chemistry of interstellar ices near 10 K in dense molecular clouds, although laboratory work on cometary-ice analogs at a similar temperature also will profit from quantification using the method we describe. We are particularly interested in the influence of H₂O-dominated ices in each case as solid H₂O is a dominant solid in cometary and interstellar ices.

2. Experimental Methods

Our laboratory work has three parts, (i) the measurement of two specific physical properties of a compound of astronomical

relevance, (ii) the use of those results to determine one or more IR intensities of the same compound in the solid state, and (iii) the measurement of the intensities of the same IR band(s) when the compound is mixed with H_2O ice. We have described the first two of these tasks in numerous papers, so only a brief summary is given here.

To determine IR band strengths of a neat (one-component) ice, we needed the ice's density (ρ) along with a reference index of refraction of the solid, both at the desired temperature and under vacuum. We used a quartz-crystal microbalance to determine densities and two-laser interferometry to measure refractive indices at 670 nm (n_{670}). In a separate measurement, we grew an ice by vapor-phase deposition onto a precooled CsI substrate, recording interference fringes during the process. The fringes and n_{670} gave the ice sample's thickness (Groner et al. 1973). An IR absorbance spectrum of the ice was then recorded in the conventional transmission mode, the IR bands of interest were integrated (resolution = 1 cm^{-1}), and the ice's density was used to calculate band strengths (Hollenberg & Dows 1961). Note that the integrated absorbance of an IR feature measured on a commercial spectrometer with a common-logarithmic (base10) scale must be multiplied by $\ln(10) \approx 2.303$ to convert it to the integrated optical depth (τ) of Equation (1). See Hudson et al. (2017) for examples, including thickness, n_{670}, density calculations, and Beer's Law plots, as well as for details concerning the IR, vacuum, and cryogenic equipment used. Readers unfamiliar with the use of Beer's Law and the extinction of light might wish to consult Hollenberg & Dows (1961) or standard texts on molecular spectroscopy (e.g., Barrow 1962; Guillory 1977), astrophysics (e.g., Böhm-Vitense 1989; Ostlie & Carroll 1996), or physical chemistry (e.g., Atkins & de Paula 2006).

The third of our three tasks, the formation of a two-component solid with H_2O ice being the more-abundant material, requires a more-detailed description. Two separate deposition lines and leak valves were connected to two glass bulbs, one holding H_2O vapor and the other with the gas of interest, leading into our sample chamber with a CsI substrate precooled to 10 K. These separate valves and lines permitted simultaneous and independent deposition of the two ice components. Knowing n_{670} and ρ for each compound allowed us to calibrate each deposition line and valve to determine the column density of each material condensing on the substrate, as outlined in the next section. No assumptions were necessary about either the flow of a gas and the quantity subsequently frozen on the substrate or about the composition in a gas-mixing bulb compared to the composition of the resulting ice sample. No reliance was necessary on liquid-phase, or other, density and refractive index measurements found in the literature. It also was not necessary to determine band strengths by forming ratios with reference IR features whose IR intensities were known or assumed. The method we have described for comparing IR band strengths of single- and two-component ices is the only novelty we claim.

All reagents used were CP grade and higher H_2S and SO_2 from Matheson and OCS from K&K Laboratories. All were used as received.

3. Band-strength Calculations

The determination of column densities is central to our method for preparing two-component ices with accurately known abundance ratios. We begin with a rearrangement of

Equation (1) to give

$$\int_{\text{band}} (\tau) d\tilde{\nu} = A'N \tag{2}$$

and then express the column density N as a product of the ice sample's number density ρ_N (molecule cm^{-3}) and thickness h to give

$$\int_{\text{band}} (\tau) d\tilde{\nu} = A'\rho_N\, h. \tag{3}$$

The number density (ρ_N) can be calculated from the mass density (ρ) we measure for each compound as

$$\rho_N = \left(\frac{N_A}{M}\right)\rho, \tag{4}$$

where N_A is Avogadro's constant and M is the molar mass of the compound. Ice thickness is found from the number (N_{fr}) of laser interference fringes recorded during the ice's growth, knowing the laser's wavelength ($\lambda = 670$ nm) and having measured the ice refractive index (n) at that wavelength. The relevant equation for our equipment is

$$h = \left(\frac{N_{\text{fr}}\lambda}{2n}\right). \tag{5}$$

Substituting Equations (4) and (5) into Equation (3), and rearranging, gives

$$\int_{\text{band}} (\tau)\, d\tilde{\nu} = A'\left[\left(\frac{N_A}{M}\right)\left(\frac{\lambda}{2}\right)\left(\frac{\rho}{n}\right)N_{\text{fr}}\right]. \tag{6}$$

Comparing Equations (2) and (6) shows that the terms in the square brackets in Equation (6) are the column density of molecules (N). Finally, because $\tau = (\ln 10)$ (absorbance), we have

$$\int_{\text{band}} (\text{Abs})\, d\tilde{\nu} = \frac{A'}{\ln(10)}\left[\left(\frac{N_A}{M}\right)\left(\frac{\lambda}{2}\right)\left(\frac{\rho}{n}\right)N_{\text{fr}}\right], \tag{7}$$

where all terms in the square brackets are known and, again, their combination gives the ice's column density, N. The conclusion from Equation (7) is that a plot of integrated absorbance as a function of the terms in the brackets (column density) should be linear with a zero intercept and a slope $A'/(\ln 10)$ from which the band strength A' can be found. In practice, with ice mixtures, we first calibrate our deposition system so that we know the rate of fringe formation for a particular setting of the deposition valve for each of the two ice components, and when making an ice mixture, we simply multiply that rate and the deposition time to get the N_{fr} used in Equation (7).

We emphasize that ρ and n must be known for an accurate calculation of the column density and hence an accurate determination of A' for an ice component. Note also that in a mixture it is still the ρ and n of each component that is needed to calculate A' and not the density and refractive index of the resulting ice.

4. Results

Table 1 summarizes the n_{670} and ρ values measured for our OCS, H_2S, and SO_2 ices at 19 K, typically the base temperature of our UHV equipment, although occasionally values as low as

Table 1
Refractive Indices and Densities Measured[a]

Compound	n_{670}	$\rho/\mathrm{g\ cm^{-3}}$
OCS	1.436	1.248
H_2S	1.407	0.944
SO_2	1.332	1.395
HCN[b]	1.346	0.850
H_2O[b]	1.234	0.719

Notes.
[a] All ices were amorphous, prepared and studied at 19 K. Values of n and ρ are averages of at least three measurements. Uncertainties are on the order of ± 0.005 and ± 0.005 g cm^{-3} for n_{670} and ρ, respectively. See the text.
[b] Values for HCN and H_2O are from Gerakines et al. (2022).

Figure 1. From top to bottom, IR spectra of amorphous ices at 10 K made from H_2O+OCS, H_2O+H_2S, and H_2O+SO_2, each with a mixing ratio of ~10:1 and a thickness of ~1 μm. Spectra are offset vertically for clarity. The broad IR bands near 3300, 2200, 1650, and 800 cm^{-1} are from H_2O ice.

16 K were reached. Each n_{670} and ρ value in Table 1 is the average of at least three determinations with standard errors on the order of 0.005 and 0.005 g cm^{-3} for n_{670} and ρ, respectively. The values of Table 1 were critical for the measurement of the band strengths of our ices, as already described. A few measurements were carried out with an older system (Moore et al. 2010), at slightly lower temperatures (~12 K), with essentially the same results (e.g., $n_{670} = 1.330$ at ~12 K versus $n_{670} = 1.332$ for SO_2 at 19 K), so that a 10–19 K temperature difference is not particularly significant for our work. The decision to use our newer ultrahigh vacuum system and the higher temperature was based on the fact that that system's microbalance permitted density measurements.

Knowing n_{670} and ρ for OCS, H_2S, and SO_2 ices, we recorded IR spectra of each compound as a function of ice thickness. Conventional Beer's Law plots were constructed, based on Equation (7), and used to derive band strengths A' for each compound at 10 K, with a focus on the stronger IR features that were unobscured by H_2O ice. Again, see our earlier papers for additional background information and typical Beer's Law graphs (e.g., Hudson et al. 2017). Readers wishing to see IR spectra of amorphous OCS at 10 K should consult Hudgins et al. (1993). Spectra of solid H_2S and SO_2 are found in Salama et al. (1990). See also our own work on OCS (Ferrante et al. 2008), H_2S (Hudson & Gerakines 2018), and SO_2 (Moore et al. 2007).

Our final task was to prepare the two-component ices H_2O+OCS, H_2O+H_2S, and H_2O+SO_2 with known column densities for the sulfur molecule in each case and to again measure integrated absorbances in each ice's IR spectrum. Figure 1 shows representative IR spectra, which agree with those of Salama et al. (1990), Hudgins et al. (1993), Moore et al. (2007), and Ferrante et al. (2008). Plotting integrated absorbance (i.e., band area) as a function of column density N gave the results shown in Figure 2, each panel representing an IR feature in an H_2O-rich ice sample. Each point in each plot is from a separate ice mixture, and three ice ratios were used in each plot. For example, in the panel for H_2O+OCS, 15 ices were examined with H_2O:OCS molar ratios of about 92:1, 9:1, and 4:1. A total of about 50 ices were used to generate Figure 2. Spectra for the three ices of Figure 1 are posted on our group's website: https://science.gsfc.nasa.gov/691/cosmicice/spectra.html.
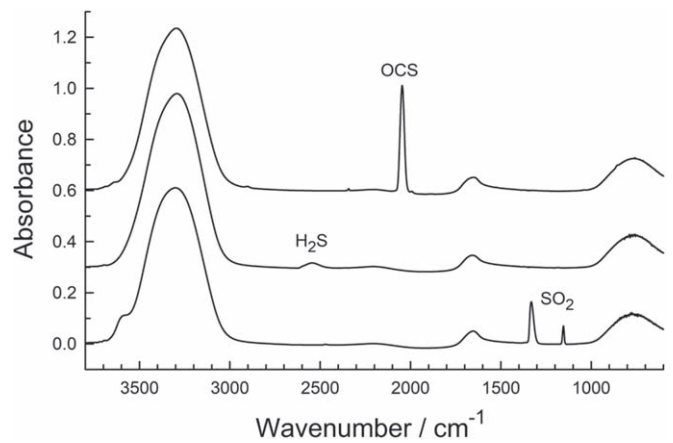
The slope of each regression line in Figure 2, after multiplication by ln (10), gives the ratio

$$\frac{\int_{\mathrm{band}} (\tau)\ d\tilde{\nu}}{N},$$

which according to Equation (1) is the band strength A', an IR intensity in a H_2O-rich ice. Such values have seldom been reported with all measurements made in a single laboratory and without the assumptions mentioned earlier.

Table 2 summarizes the band strengths we obtained for OCS, H_2S, and SO_2 in the absence and presence of H_2O ice. Results from our recent study of HCN are included for comparison (Gerakines et al. 2022). Our goal in the present work was to measure IR intensities, leaving peak positions and band shapes for a future study.

Uncertainties in A' values were estimated with both a propagation-of-error approach and a least-squares routine, taking into consideration uncertainties in both x and y quantities in the slopes of the Beer's Law plots. See both Irvin & Quickenden (1983) and Press et al. (1992). A conservative (upper) estimate for uncertainties is 5% for our A' values, which could be reduced with additional measurements. Correlation coefficients for all regression lines, such as those in Figure 2, were above 0.990.

5. Discussion

5.1. IR Band Strengths of Single-component Ices

We were motivated in our work by the question of how much band strengths might differ between one- and two-component ices, but the intensities of the single-component sulfur-containing ices, OCS, H_2S, and SO_2, are of interest in themselves.

For amorphous OCS, the only solid-phase band strengths we have located are from Hudgins et al. (1993), 1.5×10^{-16} cm molecule^{-1} and 1.7×10^{-16} cm molecule^{-1} for OCS and for an H_2O+OCS (20:1) ice, respectively. These values are larger than those in our Table 2, mainly because of the ρ and n values used by Hudgins et al. (1993). Their $\rho = 1$ g cm^{-3} was assumed for convenience, and the n used, 1.24, was based on liquid OCS, although the method of calculation was not described. The A'(OCS) later used by Palumbo et al. (1997) in a

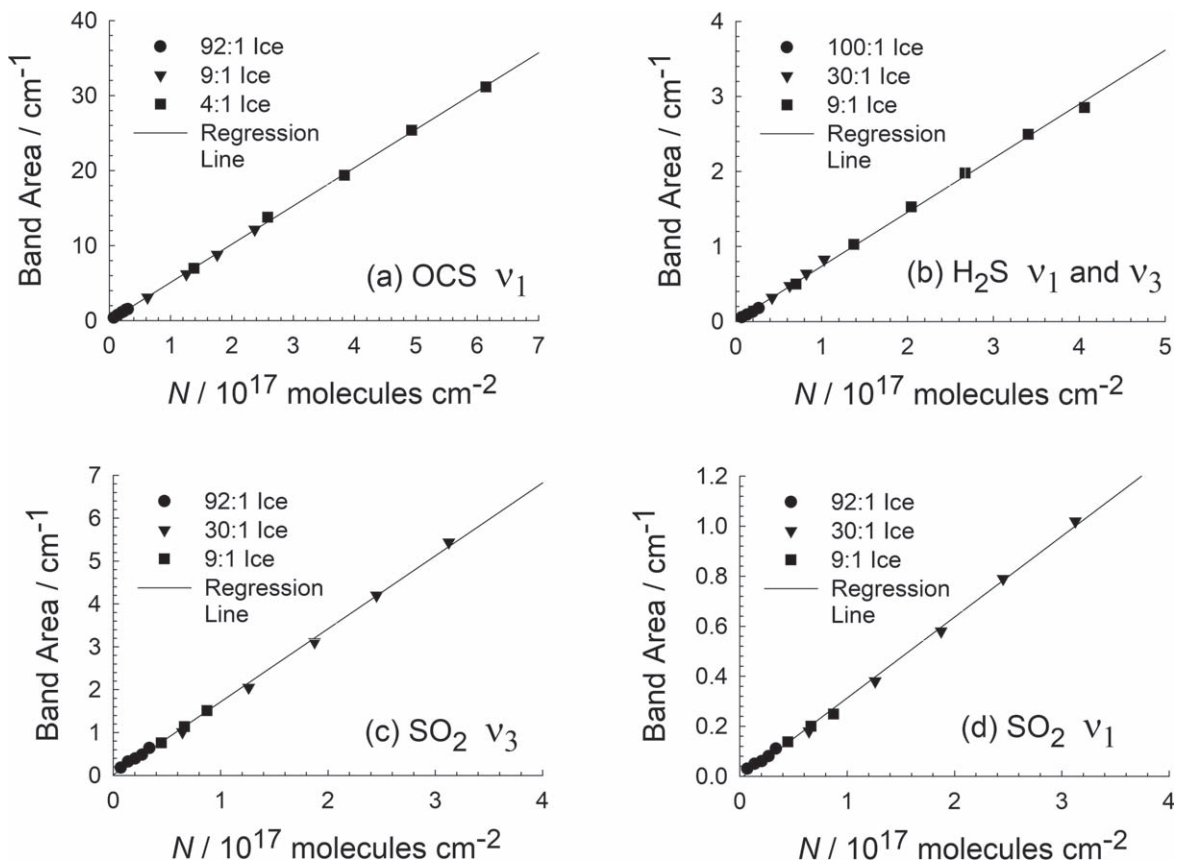**Figure 2.** IR measurements for H_2O+X ices (X = OCS, H_2S, and SO_2), with three H_2O:X ratios in each case and all spectra recorded at 10 K. Ice thicknesses ranged from about 0.2 to 1.2 μm.

study of solid OCS in dense molecular clouds was taken from Hudgins et al. (1993) and is about 25% higher than the value for neat OCS in our Table 2. This suggests that the OCS abundance in such interstellar objects is greater than the published value (i.e., a smaller value of A' in the denominator of Equation (1) raises N).

The published band strengths for amorphous H_2S also have an interesting history, which we have described in a previous publication (Hudson & Gerakines 2018). There we explained how the paper of Chen et al. (2015) adopted an $A'(H_2S)$ value from Jiménez-Escobar & Muñoz Caro (2011), who rescaled a value from Smith (1991), who used crystalline H_2S to derive a band strength that was applied to noncrystalline (amorphous) H_2S but with no statement as to the values of n and ρ adopted. Given this situation, any agreement or disagreement with our work can be regarded as little more than fortuitous. As an aside, we note that a value of $A'(H_2S)$ published some years ago by Gibb et al. (2004) is not from the paper of Salama et al. (1990) cited, but from Smith (1991).

The literature trail for SO_2 is also problematic. The SO_2 studies of Bonfim et al. (2017) and Kaňuchová et al. (2017) both refer back to earlier work by Garozzo et al. (2008) for a band strength. However, none of these three papers have details of how $A'(SO_2)$ was determined, and so any agreement or disagreement with our own work can be regarded, again, as little more than fortuitous. An earlier solid-phase study by Sandford & Allamandola (1993) applied gas-phase $A'(SO_2)$ values to amorphous SO_2 ices. Our conclusion is that, to our knowledge, the values we report for $A'(SO_2)$ in Table 2 are the first direct measurements of this band strength.

Therefore, to the question of which similar published measurements match our own, the answer is simple: none. We are unaware of any similar direct IR band-strength measurements in the literature for OCS, H_2S, and SO_2. Each of the band-strength publications cited for these compounds lacks either a pair of measured n and ρ values or details of the calculation method adopted. Moreover, integration ranges are missing in most or all cases, hindering accurate comparisons of IR band areas over the same span of wavenumbers (or wavelengths). In short, our results in Tables 1 and 2 are the first of their type for OCS, H_2S, and SO_2.

5.2. IR Band Strengths in H_2O-rich Ices—The Influence of Environment

The high degree of linearity for each panel in Figure 2 is striking and shows that the band strength A' for each compound is essentially constant over a wide range of concentrations. Table 2 lists the band strengths for the ice mixtures examined, along with the A' values for the same four compounds in the absence of H_2O ice. It is readily seen that the presence of H_2O ice in the solid sample makes relatively little difference in A'. We conclude that the A' values we measured for these compounds as neat ices are safe to use when working with H_2O-dominated mixtures.

By far the highest band strength in Table 2 is for OCS ($\sim$2040 cm^{-1}), either in the presence or absence of H_2O ice, followed by the ν_3 mode of SO_2 ($\sim$1330 cm^{-1}), and then the stretching vibrations of H_2S ($\sim$2550 cm^{-1}). The $A'(\nu_1) \approx 1.2 \times 10^{-16}$ cm molecule^{-1} for OCS is essentially

Table 2
IR Band Strengths Measured[a]

Ice	A'/cm molecule^{-1}	Integration Range/cm^{-1}	Approx. Peak Position		Mode and Approx. Description[b]
			$\tilde{\nu}$/cm^{-1}	λ/μm	
OCS	1.20×10^{-16}	2154–2070	2031	4.924	ν_1, CO stretch
H_2O+OCS	1.18×10^{-16}	2105–2070	2046	4.888	
H_2S	1.69×10^{-17}	2600–2500	2547	3.926	ν_1 and ν_3, SH stretches
H_2O+H_2S	1.66×10^{-17}	2630–2242	2545	3.929	
SO_2	4.20×10^{-17}	1400–1260	1323	7.559	ν_3, asymm stretch
H_2O+SO_2	3.92×10^{-17}	1360–1275	1332	7.508	
SO_2	7.34×10^{-18}	1165–1127	1148	8.711	ν_1, symm stretch
H_2O+SO_2	7.40×10^{-18}	1170–1135	1154	8.666	
HCN[c]	1.03×10^{-17}	2120–2070	2102	4.757	ν_3, CN stretch
H_2O+HCN[c]	1.12×10^{-17}	2120–2070	2092	4.780	

Notes.
[a] All ices were amorphous, prepared and studied at 10 K.
[b] See Shimanouchi (1972) for IR assignments.
[c] Values for HCN and H_2O+HCN are from Gerakines et al. (2022).

the same as that of the asymmetric stretch of amorphous CO_2, a commonly reported intense feature near 2340 cm^{-1} (Gerakines & Hudson 2015b). The $A'(\nu_3)$ for SO_2 is higher than that of amorphous CH_4 (Gerakines & Hudson 2015b), which also is reported in interstellar ices. Such strong IR intensities for OCS and SO_2 are in contrast to the low abundances and nondetections of these molecules in interstellar ices. Our work suggests that such small abundances and nondetections are not caused by weak IR band strengths of OCS and SO_2 but are more likely from the smaller cosmic abundance of sulfur compared to carbon and to chemical reactions, such as radiolytic oxidation, that convert S-containing molecules into SO_4^{2-} and other species that can be difficult to detect, partly due to the overlap of IR bands with other species (Moore et al. 2007). This situation resembles that of nitrogen in which cyanate (OCN$^-$) has been reported in interstellar ices, but cyanide (CN$^-$) has not (Hudson et al. 2001).

5.3. Assessment and Extensions

The method we have described for determining IR band strengths in H_2O-rich ices has the advantage of measurements being made with minimal assumptions about the composition of the ice sample. The column densities of the non-H_2O-ice and the H_2O-ice components in the mixture are derived from n and ρ values (i.e., Table 1) for each solid compound at the desired temperature, avoiding the difficulties and assumptions listed earlier. The main spectroscopic obstacle to using our approach is the usual one of overlapping IR features. Accurate integration of an IR band is difficult when an IR feature of interest is located in a region of strong absorbance by H_2O ice. This is, of course, a problem with astronomical IR spectroscopy whether laboratory or observatory based. As an example, see the extraction of a methanol abundance from the IR spectra of four protostars by Allamandola et al. (1992).

We should also mention possible laboratory complications to using the method described here. One is that vapor-phase deposition rates should be comparable in the calibration measurements on each ice component and in the two-

component ices. Related to this is that too high a deposition rate can result in the heating of an ice and structural and spectroscopic changes, as we have documented in multiple papers (e.g., Gerakines & Hudson 2015a, 2015b). Also, the ices we have studied have been on the micrometer scale. Compositions of ices of much greater thickness could be different from those of thinner solids due to thermal conductivity changes. It also is not certain if more deposition lines than the two we have used for two-component ices would be needed for quantitative studies of ices with three or more components.

Our results suggest several new lines of investigation. Perhaps first among these is the extension to other compounds. Each of the four triatomic molecules in Table 2 is polar, so experiments with NH_3, amines, and alcohols in H_2O-rich ices can also be expected to show the linearity of the plots in Figure 2. The trends for nonpolar guest molecules, such as acetylene (C_2H_2) and ethane (C_2H_6), are harder to predict. Another variation is to embed guest molecules in a nonpolar host matrix, such as solid carbon dioxide (CO_2), to see if the linear trends of Figure 2 are obtained. Finally, for applications to trans-Neptunian objects and icy satellites, our experiments should be repeated at higher temperatures, preferably after n_{670} and ρ have been measured at those temperatures. For many applications, the n and ρ values we have already published will be useful (Hudson et al. 2020).

6. Summary and Conclusions

A method for accurate determinations of IR band strengths has been described and demonstrated with OCS, H_2S, and SO_2 in amorphous H_2O-rich ice mixtures. The method described circumvents the need for a reference refractive index and density of an ice mixture.

Our measurements show that the band strengths of the stronger IR features of OCS, H_2S, and SO_2 ices hardly change when these compounds are mixed with H_2O ice at 10 K. These are the first such measurements of IR band strengths for these three sulfur compounds in the solid state.

ORCID iDs

Yukiko Y. Yarnall ⬤ https://orcid.org/0000-0003-0277-9137
Reggie L. Hudson ⬤ https://orcid.org/0000-0003-0519-9429

References

A'Hearn, M. F., Schleicher, D. G., & Feldman, P. D. 1983, ApJL, 274, L99
Allamandola, L. J., Sandford, S. A., Tielens, A. G. G. M., & Herbst, T. M. 1992, ApJ, 399, 134
Atkins, P., & de Paula, J. 2006, Atkins' Physical Chemistry (8th ed.; New York: W. H. Freeman)
Barrow, G. M. 1962, Introduction to Molecular Spectroscopy (New York: McGraw-Hill)
Böhm-Vitense, E. 1989, Introduction to Stellar Astrophysics, Vol. 1 (Cambridge: Cambridge Univ. Press)
Bonfim, V. D., Castilho, R. B., Baptista, L., & Pilling, S. 2017, PCCP, 19, 26906
Brosnan, J. T., & Brosnan, M. E. 2006, J. Nutr., 136, 1636S
Carlson, R. W., Johnson, R. E., & Anderson, M. S. 1999, Sci, 286, 97
Chen, Y. J., Juang, K. J., Nuevo, M., et al. 2015, ApJ, 798, 80
Ferrante, R. F., Moore, M. H., Spiliotis, M. M., & Hudson, R. L. 2008, ApJ, 684, 1210
Garozzo, M., Fulvio, D., Gomis, O., Palumbo, M. E., & Strazzulla, G. 2008, P&SS, 56, 1300
Gerakines, P. A., & Hudson, R. L. 2015a, ApJL, 805, L20
Gerakines, P. A., & Hudson, R. L. 2015b, ApJL, 808, L40
Gerakines, P. A., Yarnall, Y. Y., & Hudson, R. L. 2022, MNRAS, 509, 3515
Gibb, E. L., Whittet, D. C. B., Boogert, A. C. A., & Tielens, A. G. G. M. 2004, ApJS, 151, 35
Groner, P., Stolkin, I., & Günthard, H. H. 1973, JPhE, 6, 122
Guillory, W. A. 1977, Introduction to Molecular Structure and Spectroscopy (Boston, MA: Allyn and Bacon)
Heinz, J., & Schulze-Makuch, D. 2020, AsBio, 20, 552
Hollenberg, J., & Dows, D. A. 1961, JChP, 34, 1061
Hudgins, D. M., Sandford, S. A., Allamandola, L. J., & Tielens, A. G. G. M. 1993, ApJS, 86, 713
Hudson, R. L., Moore, M. H., & Gerakines, P. A. 2001, ApJ, 550, 1140
Hudson, R. L. 2016, PCCP, 18, 25756
Hudson, R. L., Loeffler, M. J., & Gerakines, P. A. 2017, JChP, 146, 0243304
Hudson, R. L., & Gerakines, P. A. 2018, ApJ, 867, 138
Hudson, R. L., Loeffler, M. J., Ferrante, R. F., Gerakines, P. A., & Coleman, F. M. 2020, ApJ, 891, 22
Irvin, J. A., & Quickenden, T. I. 1983, JChEd, 60, 711
Irwin, P. G. J., Toledo, D., Garland, R., et al. 2018, NatAs, 2, 420
Jiménez-Escobar, A., & Muñoz Caro, G. M. 2011, A&A, 536, A91
Kama, M., Shorttle, O., Jermyn, A. S., et al. 2019, ApJ, 885, 114
Kaňuchová, Z., Boduch, P., Domaracka, A., et al. 2017, A&A, 604, A68
Loeffler, M. J., Hudson, R. L., Chanover, N. J., & Simon, A. A. 2016, Icar, 271, 265
McGuire, B. A. 2018, ApJS, 239, 17
Moore, M. H., Donn, B., & Hudson, R. L. 1988, Icar, 74, 399
Moore, M. H., Ferrante, R. F., Moore, W. J., & Hudson, R. L. 2010, ApJS, 191, 96
Moore, M. H., Hudson, R. L., & Carlson, R. W. 2007, Icar, 189, 409
Ostlie, D. A., & Carroll, B. W. 1996, An Introduction to Modern Stellar Astrophysics (Reading, MA: Addison-Wesley)
Palumbo, M. E., Geballe, T. R., & Tielens, A. G. G. M. 1997, ApJ, 479, 839
Press, W. H., Teukolsky, S. A., Vetterline, W. T., & Flannery, B. P. 1992, Numerical Recipes in FORTRAN (2nd ed.; Cambridge: Cambridge Univ. Press)
Salama, F., Allamandola, L. J., Witteborn, F. C., et al. 1990, Icar, 83, 66
Sandford, S. A., & Allamandola, L. J. 1993, Icar, 106, 478
Sephton, M. 2002, Nat. Prod. Rep., 19, 292
Shimanouchi, T. 1972, Tables of Molecular Vibrational Frequencies Consolidated Volume 1, United States Department of Commerce, National Bureau of Standards, NSRDS-NBS 39 (Washington, DC: US Gov. Print. Off.)
Smith, R. G. 1991, MNRAS, 249, 172